Published in final edited form as:
Cancer Res. 2008 August 1; 68(15): 6100–6108. doi:10.1158/0008-5472.CAN-08-0540.

Neutrophil Gelatinase-Associated Lipocalin: A Novel Suppressor of Invasion and Angiogenesis in Pancreatic Cancer

Zhimin Tong[1], **Ajaikumar B. Kunnumakkara**[2], **Huamin Wang**[3], **Yoichi Matsuo**[1,6], **Parmeswaran Diagaradjane**[4], **Kuzhuvelil B. Harikumar**[2], **Vijaya Ramachandran**[5], **Bokyung Sung**[2], **Arup Chakraborty**[2], **Robert S. Bresalier**[1], **Craig Logsdon**[5], **Bharat B. Aggarwal**[2], **Sunil Krishnan**[4], and **Sushovan Guha**[1]

[1]Department of Gastroenterology, Hepatology, and Nutrition, The University of Texas MD Anderson Cancer Center, Houston, Texas

[2]Department of Experimental Therapeutics, The University of Texas MD Anderson Cancer Center, Houston, Texas

[3]Department of Pathology, The University of Texas MD Anderson Cancer Center, Houston, Texas

[4]Department of Radiation Oncology, The University of Texas MD Anderson Cancer Center, Houston, Texas

[5]Department of Cancer Biology, The University of Texas MD Anderson Cancer Center, Houston, Texas

[6]Department of Gastroenterological Surgery, Nagoya City University Graduate School of Medical Sciences, Nagoya, Japan

Abstract

Neutrophil gelatinase associated lipocalin (NGAL) is a 25 kDa secreted acute phase protein, which is also upregulated in multiple cancers, including breast, lung, and pancreas. Recently, NGAL has been proposed as an early biomarker in pancreatic cancer (PaCa). However, its biological role in PaCa is unknown. In this study, we examined *in vitro* and *in vivo* functional role of NGAL in PaCa. Well to moderately differentiated PaCa cells (AsPC-1, BxPC-3, and Capan-2) expressed high levels of NGAL but moderate to poorly differentiated PaCa cells (PANC-1 and MIAPaCa-2) expressed undetectable NGAL levels. Immunohistochemistry of untreated tissue microarray showed specific NGAL staining in resected PaCa specimens ($p=0.0167$). Stable NGAL overexpression (MIAPaCa-2 and PANC-1) significantly blocked PaCa cells adhesion and invasion *in vitro* and *vice versa* with stable NGAL-shRNA PaCa clones (BxPC-3 and AsPC-1). Moreover, NGAL overexpression reduced focal adhesion kinase (FAK) tyrosine-397 phosphorylation in PaCa cells. Further, NGAL overexpression potently decreased angiogenesis *in vitro* partly through reduced VEGF production and *vice versa*. Stable NGAL over- or underexpression had no effects on PaCa cell survival, viability, and response to chemotherapeutic drugs. Finally, MIAPaCa-2 cells overexpressing NGAL reduced tumor volume ($p=0.012$), local and distant metastasis ($p=0.002$), and angiogenesis ($p=0.05$) with no effect on K-67 proliferation index ($p>0.1$) in an orthotopic nude mouse PaCa model. Collectively, our results suggest that NGAL reduces adhesion/invasion partly by suppressing FAK activation and inhibits angiogenesis partly by blocking VEGF production in PaCa cells. Thus, NGAL is a potential suppressor of invasion and angiogenesis in advanced PaCa.

Address for reprints: Sushovan Guha, MD, PhD; Department of Gastroenterology, Hepatology, and Nutrition; Unit 436, 1515 Holcombe Boulevard; Houston, TX 77030; Phone: 713-745-7566; Fax: 713-563-4398; E-mail: E-mail: sguha@mdanderson.org.

Keywords

NGAL; lipocalin 2; invasion; angiogenesis; pancreatic cancer

BACKGROUND

Neutrophil gelatinase associated lipocalin (NGAL), also called lipocalin-2, belongs to the lipocalin protein family and was first purified from human neutrophils because of its association with gelatinase (1). NGAL exists as a 25-kDa monomer, 46-kDa disulfide-linked homodimer, and 135-kDa disulfide-linked heterodimer with neutrophil gelatinase (2). NGAL is an immuno-modulator since its expression is upregulated in humans, typically in epithelial cells, under diverse inflammatory conditions, including appendicitis, inflammatory bowel disease, and diverticulitis (3). NGAL is also able to inhibit microorganism growth by interfering with siderophore-mediated iron acquisition (4). Moreover, NGAL can protect against acute ischemic renal injury and plays a role in cell survival (5,6).

Elevated NGAL expression has also been observed in multiple human cancers including breast, colorectal, and ovarian cancers; however, the biological roles of elevated NGAL in cancer cells are not yet clear (3,7–9). Recently, it was reported that NGAL suppressed cellular invasion and metastases in colon cancer and in Ras-transformed mouse mammary cells *in vitro* (10, 11). In contrast, NGAL is able to facilitate gastrointestinal mucosal regeneration by promoting cell migration (12). In breast cancer, NGAL expression is considered as a poor prognostic marker and is associated with invasive properties (13). However, in ovarian cancer, NGAL expression blocked epithelial to mesenchymal transition, one of the hallmarks of invasive neoplasia (8).

Multiple clinical studies have identified NGAL as a selective and an early biomarker in pancreatic cancer (PaCa) tissues using gene expression analyses (14–19). Recently, proteomic analysis of pancreatic exocrine secretions have also confirmed NGAL expression in PaCa (20). Given the fact that PaCa is the most deadly gastrointestinal cancer in the western countries with poor survival rates (21), it is of utmost importance to understand the role of NGAL in this inevitably fatal disease. But, to date, nothing is known regarding NGAL functions in PaCa.

In the current study, we examined biological functions of NGAL in PaCa cells. We observed significant reduction in PaCa cells adhesion, invasion, and angiogenesis by NGAL overexpression and *vice versa*. Reduction of NGAL-induced cellular invasion is in part due to inhibition of FAK phosphorylation and reduction of angiogenesis is in part due to inhibition of VEGF secretion by these cells. However, we did not detect any effects of NGAL over- or under-expression on cell proliferation, survival, and sensitivity to chemotherapeutic agents. Finally, we showed that NGAL overexpression in an orthotopic model of PaCa significantly inhibited local/distant metastasis and reduced tumor microvessel density.

MATERIALS AND METHODS

Cell lines and culture conditions

Human PaCa cell lines (AsPC-1, BxPC-3, Capan-2, PANC-1, and MIAPaCa-2) and human umbilical vascular endothelial cells (HUVEC) were purchased from ATCC and Lonza (Walkersville, MD) respectively. HPV-E6/E7 immortalized human pancreatic ductal epithelial (HPDE) cell line was a kind gift from Dr. M. S. Tsao (22). AsPC-1, BxPC-3 and Capan-2 were cultured in RPMI-1640 medium supplemented with 10% FBS and antibiotics (100 μg/ml streptomycin and 100 IU/ml of penicillin). PANC-1 and MIAPaCa-2 were cultured in Dulbecco's Modified Eagle Medium (DMEM) supplemented with 10% FBS and antibiotics.

HUVEC cells were cultured in endothelial growth medium-2 (EGM-2) (Lonza). 293FT cells (from Invitrogen, Carlsbad, CA) were maintained in DMEM supplemented with 10 % FBS and 500 μg/ml G418. HPDE cells were cultured in Keratinocyte-SFM medium supplemented with 50 μg/ml of bovine pituitary extract and 5 ng/ml of recombinant EGF (Invitrogen, Carlsbad, CA). Cells were passaged at 80% confluency using 1 mM EDTA-0.025% trypsin for 3 to 5 minutes.

Reagents and treatments

5-FU was purchased from Calbiochem (San Diego, CA). Gemcitabine (Gemzar) was kindly supplied by Eli Lilly Co (Indianapolis, IN). Plasmids (pLenti-L6H with fulllength NGAL and pLL3.7B-shNGAL) were gifts from Dr. Jang-Seong Kim (Mogan Biotechnology Research Institute, Yongin-city, Republic of Korea). Mouse monoclonal NGAL antibody was purchased from Antibody Shop (Gentofte, Demark). FAK, phospho-FAK, XIAP, and survivin antibodies were obtained from BD Biosciences (Franklin Lakes, NJ). Antibodies to cMyc, cyclin D1, cIAP1, TRAF1, Bcl-xL, and Bcl-2 were purchased from Santa Cruz Biotechnology, Inc. (Santa Cruz, CA). Formalin-fixed, paraffin-embedded (FFPE) tissue microarray slides of human PaCa were obtained from the Department of Pathology at UTMDACC. 5-FU was dissolved in DMSO and gemcitabine was dissolved in sterile PBS. Rest of the reagents used was of highest quality.

Cell viability assay

Cell viability was measured using the CellTiter Aqueous One Solution Cell Proliferation Assay kit (Promega, Madison, WI). Briefly, treated or untreated cells were incubated with the reaction solution for 2 h at 37°C. The absorption at 490 nm was measured using a microplate reader. The results are presented as the percentage of controls.

Cell apoptosis assay

Cells were harvested, washed with cold PBS, resuspended in a solution containing 5 μl of recombinant Annexin V-FITC (Caltag, Burlingame, CA) and 5 μg/ml of propidium iodide, and incubated for 15 minutes. Cells were analyzed with a Coulter F500 flow cytometer equipped with an argon laser (excitation wavelength of 488 nm and emission wavelengths used for propidium iodide and Annexin V were 620 and 525 nm, respectively). Cells stained with propidium iodide alone were considered necrotic, whereas cells stained with Annexin V were considered apoptotic.

Western blot

Proteins in the culture medium or cell lysates were separated by 10% or 12% SDS-PAGE. The separated proteins were electrophoretically transferred to Immobilon™ transfer membranes (Millipore, Bedford, MA) and incubated with a blocking solution, 5% dry milk in TBST (25 mM Tris-HCl, pH 7.6, 200 mM NaCl, 0.15% Tween 20), for 1 hour at room temperature. Target protein levels were measured by immunoblotting with the corresponding antibodies. Blots were washed 3 times for 15 minutes each time at room temperature with TBST and then incubated for 1 hour with secondary anti-mouse or anti-rabbit peroxidase-linked antibodies (1:10000, Amersham, Piscataway, NJ) in a blocking solution. Blots were then washed (3 × 15 minutes). Bands were visualized by enhanced chemiluminescence (ECL) (Amersham, Piscataway, NJ).

RNA isolation and RT-PCR

Total RNA from cells was isolated using the RNeasy mini kit (Qiagen, Valencia, CA). RT-PCR was performed using a one-step kit (Invitrogen) for 35 cycles at 94°C for 15 s, 55°C for 30 s, and 72°C for 45 s. NGAL primer was designed using Primer3 software according to the sequence of the NGAL gene (accession number: X83006) and β-actin primers were used as

loading control. The amplified PCR products were resolved by 1.5% agarose gel electrophoresis containing ethidium bromide.

Generation of stable NGAL overexpression or NGAL-shRNA PaCa Cell Lines

To produce lentivirus for NGAL overexpression or NGAL-shRNA (shNGAL), pLenti-L6H plasmid or pLL3.7B-shNGAL plasmid respectively, and control vector were co-transfected with ViroPower Packaging Mix into 293FT cells by using lipofectamine 2000 reagent (Invitrogen). Medium containing lentivirus with NGAL overexpression or underexpression was used to transduce PaCa cells 48 h after transfection. After transduction, cells with stable expression of NGAL overexpression or shNGAL were selected by incubation in a medium containing blasticidin for at least 2 weeks. NGAL expression of stable cell lines was further confirmed by western blots.

Adhesion assay

The adhesion assay was performed by using an adhesion chamber. A coverslip coated with fibronectin (1 μg/ml) was placed in the bottom of the adhesion chamber, and another plain coverslip was placed on the top of that, separated by a rubber O-ring. A cell suspension (1×10^5/ml in culture medium) was injected into the chamber. Cells that were seeded onto the fibronectin-coated coverslip were counted under an inverted microscope in 10 random low-power fields (40x) as the base number. After 10 minutes, the chamber was inverted and the cells bound to the fibronectin-coated surface were again counted in 10 random 40x fields. The adhesion of cells was recorded as the percentage of the base number at seeding.

Invasion assay

The invasion capability of cells was determined by using a Matrigel™-coated invasion chamber with 0.8-μm pore (BD Biosciences, Franklin Lakes, NJ). A single cell suspension (200 μl) containing 1×10^5 cells was added to the inner chamber after the addition of 600 μl of culture medium to the bottom chamber. Following 16 h of incubation at 37°C in 5% CO_2, cells on the upper surface of the inner chamber were removed with cotton swabs. Invaded cells that adhered on the lower surface of the membrane were fixed, stained with Diff-Quik (Dade Behring, Newark, DE), and counted.

HUVEC tube formation assay

HUVEC (1×10^4) in 100 μl of diluted conditioned medium (1:1 dilution) from NGAL overexpression or shNGAL clones were seeded onto 96-well plates that were pre-coated with Matrigel™ for 1 hour. After 16 h, the total number of vascular tubes were counted under a microscope.

ELISA

Cells were cultured in a 100-mm dish (1.5×10^6 cells/dish) with 9 ml of culture medium containing 2% fetal bovine serum for 24 h. The levels of VEGF in the culture medium were assayed by using a commercially available VEGF ELISA kit (R&D Systems, Minneapolis, MN).

Immunohistochemistry

FFPE slides were deparaffinized and immunohistochemistry (IHC) was performed as previously described (23). Monoclonal NGAL antibody (1:10) was used. Slides were developed with DAB solution (Dako, Carpenteria, CA) for 2–5 minutes and counterstained with Harris's hematoxylin for 10 s. The presence of brown color indicated a positive staining of NGAL.

Ki-67 analysis

FFPE sections (5 μm) were stained with Ki-67 (rabbit monoclonal clone SP6, NeoMarkers, Fremont, CA) antibody as previously described (23). Results were expressed as percent of $Ki\text{-}67^+$ cells ± SE per 40x magnification. A total of 10 fields (40x) were examined and counted from each treatment groups (n = 5/group). The values were compared using unpaired Student's *t-test*.

Microvessel density

OCT fixed cryo-sections (5 μm) were stained with rat anti-mouse CD31 monoclonal antibody (BD Biosciences) as previously described (23). Areas of greatest vessel density were then examined under higher magnification (100x) and counted. Results were expressed as the mean number of vessels ± SE per high power field (HPF or 100x). A total of 20 HPFs were examined and counted from each treatment groups (n = 5/group). The values were compared using unpaired Student's *t-test*.

Animals

Male athymic *nu/nu* mice (4 weeks old) were obtained from the breeding colony of the Department of Experimental Radiation Oncology at UTMDACC. Before initiating the experiment, we acclimatized all mice to a pulverized diet for 3 days. Our experimental protocol was reviewed and approved by the Institutional Animal Care and Use Committee (IACUC) at UTMDACC.

Orthotopic pancreatic cancer model

MIAPaCa-2 cells stably transfected with NGAL and corresponding control vector were stably transduced with luciferase as previously described (24,25). The animals were divided into 2 groups (n = 5/group). The first group was injected with MIAPaCa-2 cells that are transfected only with vector and the second with MIAPaCa-2 cells that are transfected with NGAL. Mice were anesthetized with ketamine-xylazine solution, a small left abdominal flank incision was made, and (1×10^6) MIAPaCa-2 cells in 100 μL PBS were injected into the subcapsular region of the pancreas using a 27-gauge needle and a calibrated push button-controlled dispensing device (Hamilton Syringe Company, Reno, NV). The abdominal wound was closed in one layer with wound clips (Braintree Scientific, Inc.; Braintree, MA).

Experimental protocol

One week after implantation, tumor volumes were monitored weekly by IVIS 200 (Xenogen, Alameda, CA) using a cryogenically cooled bioluminescence imaging system coupled to a data acquisition computer running Living Image software (Xenogen) as previously described (24, 25). Mice were imaged on days 7, 14, 21, and 28 after tumor cells implantation. The animals were sacrificed on 35^{th} day after tumor cell implantation. Primary tumors in the pancreas were excised and the final tumor volume was measured as $V = 2/3\ \pi r^3$, where r is the mean of the three dimensions (length, width, and depth). All the measurements were compared amongst 2 groups using unpaired Student's *t-test*. Half of the tumor tissue was formalin-fixed and paraffin-embedded for IHC (Ki-67) and routine H&E staining. The other half was divided into 2 sections: one portion snap-frozen in liquid nitrogen and stored at −80°C and the other part fixed in OCT and then preserved for cryo-sections (CD31). H&E staining confirmed the presence of tumor(s) in each pancreas.

RESULTS

NGAL expression in PaCa

To examine NGAL expression in human PaCa tissues, we performed immunohistochemical staining of formalin-fixed paraffin-embedded tissue microarrays with anti-NGAL antibodies (Fig. 1A). We found that only 45% of PaCa tissues exhibited strong luminal and cytosolic staining of NGAL. Interestingly, 26% of adjacent chronic pancreatitis sections also showed NGAL staining. However, normal pancreatic ductal epithelial cells expressed no NGAL. Amongst PaCa staining, NGAL was detected predominantly in PanIN-1 and PanIN-2 lesions (data not shown).

The NGAL expression in PaCa cells was next evaluated by RT-PCR using total RNA extracted from 5 PaCa cell lines and NGAL-specific primers. As shown in Fig. 1B, all 5 cell lines expressed NGAL. However, the expression of NGAL was dramatically higher in Capan-2, BxPC-3, and AsPC-1 cells than in MIAPaCa-2 and PANC-1 cells. To confirm this result, cell lysates and condition medium from these cells were subjected to western blot with anti-NGAL antibodies (Fig. 1C). Consistent with the RT-PCR results, Capan-2, BxPC-3 and AsPC-1 cells had high levels of both NGAL expression and secretion. However, the expression and secretion of NGAL at MIAPaCa-2 and PANC-1 cells were undetectable, as well as in immortalized HPDE cells (data not shown).

Generation of NGAL over-expressing and under-expressing PaCa cells

MIAPaCa-2 and PANC-1 cells with low basal NGAL expression were stably transduced with lentivirus overexpressing NGAL, designated as MIA-NGAL and PANC-NGAL, respectively. The expression of NGAL was detected by western blotting. As shown in Fig. 2, MIA-NGAL and PANC-NGAL had very high levels of NGAL expression and secretion, whereas levels of NGAL expression and secretion were undetectable in control MIAPACA-2 and PANC-1 cells (designated as MIA-mock and PANC-mock). In addition, we also generated lentivirus-mediated stable expression of NGAL-shRNA in AsPC-1 and BxPC-3 cells with high basal NGAL expression, designated as AsPC-shNGAL and BxPC-shNGAL, respectively. The downregulation of NGAL was also confirmed by western blotting (Fig. 2).

Effects of NGAL on cell adhesion and invasion

Based on previous studies showing NGAL significantly inhibited metastasis in colon cancer (11) and blocked invasion of *H-Ras*-transformed 4T1 mammary cells (10), we investigated its possible role in PaCa cell adhesion and invasion. We first examined the adhering ability of PaCa cells that overexpress either NGAL or shNGAL by using fibronectin-coated adhesion chambers. We observed that the adhesion rates of MIA-mock and MIA-NGAL cells were 82.8 ± 2.7% and 52.2 ± 3.7%, respectively, after 10 min of adherence to fibronectin (Fig. 3A, left panel). In contrast, the adhesion rates of BxPCmock and BxPC-shNGAL cells were 54.1 ± 8.8% and 99.2 ± 0.8 %, respectively (Fig. 3A, right panel). Thus, NGAL blocked adhesion of PaCa cells to fibronectin-coated surface.

Next, we investigated whether NGAL blocked invasive capabilities of PaCa cells through Matrigel™. We showed that NGAL overexpression suppressed the ability of MIAPaCa-2 cells to invade through Matrigel™ by 55.7 ± 14% (Fig. 3B, left panel). Conversely, NGAL downregulation increased BxPC-3-shNGAL cellular invasion through Matrigel™ by 27 ± 1% (Fig. 3B, right panel). Our results indicate that NGAL plays a significant role in adhesion and invasion of PaCa cells.

Effect of NGAL on FAK activation

Focal adhesion kinase (FAK) is an important regulator of cell adhesion and invasion (26). Having demonstrated that NGAL overexpression inhibits PaCa cell adhesion and invasion, we sought to determine whether FAK activation was altered in these cells. Activation of FAK requires tyrosine phosphorylation at 397 (Y397) (26). Therefore, we examined FAK activation by western blotting using phospho-Y397-FAK specific antibody. As shown in Fig. 3C, MIA-NGAL cells exhibited decreased level of FAK phosphorylation compared with MIA-mock cells. In contrast, BxPC-shNGAL cells had higher levels of FAK phosphorylation than did BxPC-mock cells. These results suggest that NGAL regulates cell invasion in part through the regulation of FAK phosphorylation.

Effects of NGAL on HUVEC tube formation *in vitro*

A previous report showed that NGAL blocked angiogenesis in *H-Ras*-transformed 4T1 cells (27), thus indicating a possible role of NGAL in PaCa angiogenesis. To determine the effects of NGAL on angiogenesis, conditioned media from MIA-NGAL, and PANC-NGAL cells (containing high amounts of NGAL) and from BxPC-3-shNGAL (containing reduced NGAL) were used to assay for tube formation of HUVEC cells on Matrigel™. Conditioned media from MIA-NGAL (Fig. 4A) and PANC-NGAL (Suppl. Fig. 2B) significantly reduced the tube formation of HUVEC cells, by 69.5 ± 5% and 68 ± 7.5%, respectively, compared with the conditioned media from their control cells. In contrast, conditioned media from BxPC-shNGAL increased the tube formation by 63.5% (Fig. 4B). Thus, our results confirm that NGAL inhibits HUVEC tube formation.

Effect of NGAL on VEGF production

As vascular endothelial growth factor (VEGF) is a key molecular mediator of angiogenesis, we investigated whether NGAL could regulate VEGF production. To evaluate this possibility, we used an ELISA with conditioned media from PaCa cells either overexpressing NGAL or NGAL-shRNA. VEGF secretions from MIA-NGAL and PANC-NGAL were 49% reduced ($p<0.05$) as compared to MIA-mock and PANC-mock (Fig. 4C and Suppl. Fig. 2C). Interestingly, addition of VEGF to the conditioned media was not able to rescue HUVEC tube formation (Suppl. Fig. 2D). NGAL downregulation in BxPC-3 cells (BxPC-shNGAL) significantly increased secretion of VEGF by 30.3% ($p<0.05$) as compared to controls (Fig. 4D). These data indicate that NGAL potently blocks PaCa angiogenesis *in vitro* in part through reduction of VEGF secretion.

Effects of NGAL on proliferation and viability of PaCa cells

Pervious studies showed that NGAL can stimulate cell proliferation (28) and tumor growth (29). We therefore investigated whether NGAL can affect PaCa cell proliferation and viability. No difference in cell proliferation was observed between MIA-NGAL and control, as determined by the CellTiter AQ assay (Fig. 5A). Similar results were obtained with PANC-NGAL cells (data not shown). Cell proliferation of BxPC-shNGAL also did not differ from that of BxPC-3-mock cells (Suppl. Fig. 3A).

To further investigate whether manipulation of NGAL expression could affect cell viability, we measured apoptosis of MIA-NGAL, PANC-NGAL, AsPC-shNGAL, and BxPC-shNGAL and their corresponding control cells by flow cytometry following staining with Annexin V-FITC. Similar to the results for cell proliferation, upregulation or downregulation of NGAL had no effect on cellular apoptosis (Fig. 5B).

Western blots also confirmed no significant difference in the expression pattern of multiple proteins related to cell proliferation (c-Myc and cyclin D1), apoptosis, and survival (cIAP1,

XIAP, survivin, TRAF-1, Bcl-xL, and Bcl-2) between PaCa cells with either upregulation or downregulation of NGAL and their corresponding controls (Fig. 5C).

Effects of NGAL on PaCa cells sensitivity to chemotherapy

PaCa cells are inherently resistant to chemotherapy (30). Because NGAL is able to protect cells from the toxicity of certain chemicals (12) and apoptosis inducers (6), we sought to determine whether elevated NGAL expression in early PaCa plays a role in sensitivity to conventional chemotherapy. To test this idea, we treated cells with NGAL overexpression, NGAL-shRNA, or control vector with an increasing dose of gemcitabine for either 48 h (BxPC-3) or 72 h (MIAPaCa-2). PaCa cell toxicity to gemcitabine was then determined by using the CellTiter AQ assay. We observed that sensitivity of PaCa cells with either upregulated or downregulated NGAL to gemcitabine did not differ from that of their controls (Fig. 5D and Suppl. Fig. 3B). Similar results were observed for 5- FU treatment (data not shown).

Effects of NGAL on PaCa growth and metastases *in vivo*

Next we examined whether NGAL overexpression can inhibit PaCa growth, angiogenesis, and metastases *in vivo*. We used MIAPaCa-2 cells either overexpressing NGAL (MIA-NGAL) or control vector (MIA-vector) stably transduced with luciferase for real-time bioluminescence imaging in order to monitor tumor volume and spread *in vivo* (Suppl. Fig. 4A and Suppl. Fig. 4B). These cells were then orthotopically injected into the body of the pancreata of nude mice and a week later, bioluminescence imaging was started once per week. Fig. 6A (left panel) indicated the representative bioluminescence images of MIA-vector and MIA-NGAL on days 7, 14, 21, and 28 after orthotopic injection. Fig. 6A (right panel) showed the significant difference ($p = 0.05$) in the bioluminescence area between the 2 groups ($n = 5$ per group). At the end of 35^{th} day, the mice were euthanized and the final tumor volume was measured. As shown in Fig. 6B (left panel), MIA-NGAL tumors were significantly smaller than MIA-vector ($p = 0.012$). We calculated the metastasis score by tabulating the total number of visually recognizable of metastatic foci in liver, omentum/mesentery, and spleen per mouse after careful dissection. Fig. 6B (right panel) demonstrated the striking reduction in the metastasis score of MIA-NGAL group as compared with MIA-vector ($p = 0.002$). Next, we showed no difference in proliferation index amongst the 2 groups as determined by Ki-67 immunohistochemistry (Fig. 6C and Suppl. Fig. 4C). However, there is a reduction in the microvessel density of MIA-NGAL tumors compared with control ($p = 0.05$) as determined by $CD31^+$ staining of tumor explants (Fig. 6D and Suppl. Fig. 4D). Collectively, our data indicates that NGAL overexpression reduced tumor volume, angiogenesis, and metastatic spread of PaCa *in vivo*.

DISCUSSION

NGAL, a member of the lipocalin family (1), is upregulated in a number of pathological conditions, including cancers (3). However, its importance in cancer progression remains unknown. In the current study, we investigated expression of NGAL in PaCa and possible roles of NGAL in PaCa progression. The main findings of the present study demonstrate that significant increase in NGAL expression occurs in the early stage of PaCa development and that overexpression of NGAL blocks cell adhesion, invasion, and angiogenesis of PaCa.

NGAL was described as a biomarker of cancer progression because of the association of increased NGAL expression with estrogen receptor-negative breast cancer cells (31). In addition, upregulated NGAL expression was found only in the early stage of ovarian cancer (8). Our current study also suggests that NGAL could act as a biomarker for early stages of PaCa, as evidenced by the fact that well- to moderately-differentiated PaCa cells (AsPC-1, BxPC-3, and Capan-2 cell lines) had very high levels of NGAL expression and secretion, whereas NGAL expression and secretion of poorly differentiated PaCa cell lines (MIAPaCa-2

and PANC-1) were undetectable. Furthermore, IHC showed that only 45% of surgically resectable PaCa tissues were NGAL positive. NGAL expression significantly increases in early PaCa but progressively gets reduced in late PaCa. We are currently investigating whether *loss of NGAL* expression in late stages is a potential biomarker of locally advanced/metastatic PaCa. Due to small sample size, we didn't observe any significant association between NGAL expression and stage or differentiation status of PaCa. We also observed NGAL expression in ducts from adjacent chronic pancreatitis (CP) tissues. This is in agreement with earlier reports that NGAL is an inflammation-induced protein in multiple cell types (4). But it is not known whether NGAL expression in CP can predict further development of progressive advanced PanIN lesions that are pathognomonic of PaCa tissues (32).

Our current study demonstrated that NGAL overexpression reduced PaCa cell adhesion and invasion *in vitro* and *in vivo*. In support of this idea, Lee *et al* (11) reported that overexpression of NGAL blocked human colon cancer KM12SM cell invasion and liver metastasis. In contrast, Li *et al* (33) reported that downregulation of NGAL by antisense suppressed human esophageal carcinoma SHEEC cell invasion *in vivo*. These apparently conflicting observations could be due to distinct functions of NGAL in different cell types. One key difference is that the anti-invasive properties of NGAL noted are predominantly in oncogenic *K-Ras* mediated transformed cells (colon and PaCa) unlike SHEEC, which was transformed by phorbol ester. This is further supported by a previous study showing that NGAL overexpression also suppressed Ras-transformed murine breast cancer 4T1 cell invasion and lung metastasis *in vivo* (10). Interestingly, in a study of gastrointestinal mucosal integrity and repair, administration of exogenous NGAL facilitated mucosal regeneration by promoting cell migration (12). This indicates that NGAL functions differently in the context of mucosal restitution.

The mechanisms by which NGAL regulates tumor metastasis are unclear. Study in human esophageal carcinoma SHEEC cells suggested that NGAL downregulation suppressed cell invasion through reduction in MMP-9 activity (33). Overexpression of NGAL blocked Ras-transformed murine breast cancer 4T1 cell invasion and metastasis, possibly through the suppression of Ras-induced E-cadherin phosphorylation and subsequent inactivation (10). In PaCa, effects of NGAL on cell invasion are partly mediated through the regulation of FAK phosphorylation. This is supported by the fact that manipulation of NGAL expression altered FAK phosphorylation at residue Y397, which is critical for FAK activation. Future studies will address the mechanism by which NGAL regulates FAK activation in PaCa. Furthermore, upregulation or downregulation of NGAL did not change the activity of MMP-9 in PaCa (Z. Tong and S. Guha, unpublished observation). It is well known that FAK, a 125-kDa cytoplasmic tyrosine kinase, is an important molecule involved in tumor invasion and metastasis, including PaCa. For instance, downregulation of FAK by RNA interfering inhibits the metastasis of human pancreatic adenocarcinoma cells (34). In addition, periostin promotes CFPanc1 PaCa cell invasion by an increase in the phosphorylation of FAK (35). Furthermore, FAK forms complexes with integrins and integrin-linked kinase (ILK). These complexes are also critical for mediating cellular adhesion, migration, and invasion. NGAL could potentially interact with FAK-integrin complexes either directly or indirectly and thereby affect migration and invasion of PaCa cells. Thus, FAK signaling pathways either directly or indirectly through interactions with integrin complexes may play a significant role in mediating effects of NGAL on PaCa invasion.

In addition to the involvement in metastasis, the results of our study also indicate that NGAL can inhibit angiogenesis in PaCa cells, both *in vitro* and *in vivo*. This is in agreement with a previous report in Ras-transformed 4T1 cells (27). It is well known that the angiogenic process depends on a net balance of positive and negative angiogenic factors in the tumor. One of the key molecules involved in angiogenesis is VEGF (36). PaCa cells overexpress a number of

pro-angiogenic factors, including VEGF (37). An important mechanism by which NGAL overexpression may reduce PaCa angiogenesis is partly through the reduction of VEGF production or through blockade of VEGF action on HUVEC. NGAL could directly or indirectly interact with VEGF in the conditioned medium and prevents VEGF-VEGFR2 mediated signaling in HUVEC. In addition, perturbations of FAK-integrin mediated signaling events could also lead to reduced HUVEC tube formation. Similarly, overexpression of NGAL dramatically suppressed Ras-induced VEGF production in 4T1 cells (27). Further studies will delineate whether the effects are at the transcriptional, translational, or post-translational level of regulation. Of course, involvement of other angiogenic factors in NGAL mediated inhibition of PaCa angiogenesis cannot be excluded.

One of the salient features in this manuscript was validation of *in vitro* data on NGAL overexpression mediated reduction in invasion and angiogenesis in our orthotopic mouse model of PaCa. As expected, NGAL effects on tumor cell proliferation were not significant ($Ki\text{-}67^+$ cells) but we observed a modest reduction in the final tumor volume. This could be attributed in part to the reduction in angiogenesis as observed by reduction in tumor microvessel density ($CD31^+$ cells). However, one cannot rule out the possibility that effects of NGAL on cell proliferation and/or apoptosis are dependent on cellular growth in a defined basement membrane or in an anchorage-independent manner. But the striking observation was the suppression of local and distant metastases by NGAL overexpression *in vivo*. Further, using green and red fluorescent orthotopic models of PaCa metastasis *in vivo* (38–40), we will validate our findings with NGAL overexpression and underexpression clones. Taken together, our results suggest that NGAL could regulate multiple proteins including FAK-integrin signaling pathways, which play a significant role in the process of metastasis *in vivo*.

Accumulated evidence indicates that NGAL plays roles in the regulation of cell growth. For instance, upregulated NGAL was highly correlated with the S-phase fraction in breast cancer (9), overexpresssion of NGAL stimulated breast tumor growth *in vivo* (29), and administration of exogenous NGAL to ischemic injured kidney resulted in the enhanced tubule cell proliferation (28). In PaCa, however, NGAL had no effects on cell proliferation, given that overexpression or downregulation of NGAL did not change cell growth. Similar results were also reported in colon cancer (11). Thus the effects of NGAL on cell proliferation may be cell type specific and context dependent.

NGAL is thought to be a survival factor due to induction of cellular apoptosis by NGAL antibody and increase in cellular resistance to PDK1 inhibitor by NGAL overexpression in lung cancer A549 cells (6). In MCF-7 breast cancer cells, upregulation of NGAL also makes cells more resistant to the chemotherapeutic agent 4-HRP (41). However, data from the current study showed that NGAL has no effects on the viability of PaCa cells or their sensitivity to chemotherapeutic agents, since the manipulation of NGAL expression, either upregulation or downregulation of NGAL expression, resulted in no changes in cell apoptosis or in gemcitabine-induced cell death compared with control cells. Similarly, apoptosis induced by several apoptotic inducers in thymocytes isolated from $Lcn2^{-/-}$ mice had no significant different from that in wild type (WT) thymocytes (42). Therefore, the effect of NGAL on cell sensitivity to chemotherapeutic agents may depend on the nature of the chemicals or cell type. That downregulation of NGAL did not result in significant cellular apoptosis in the current study could also be due to the incomplete silencing of NGAL, which is enough to maintain cell viability.

In summary, well to moderately differentiated PaCa cells and few resected PaCa tissues showed upregulated NGAL expression. Overexpression of NGAL had no effects on PaCa cell viability or sensitivity to chemotherapy but did block PaCa cell adhesion, invasion, and angiogenesis. The involvement of NGAL in cell invasion and angiogenesis may be through the alteration of

FAK phosphorylation and VEGF production, respectively. Therefore, *loss* of NGAL is a biomarker of PaCa progression, and manipulation of NGAL expression could control PaCa angiogenesis and metastasis.

Supplementary Material

Refer to Web version on PubMed Central for supplementary material.

Abbreviations

FBS, Fetal bovine serum; VEGF, vascular endothelial growth factor; EGF, epidermal growth factor; UTMDACC, The University of Texas MD Anderson Cancer Center; NGAL, Neutrophil gelatinase associated lipocalin.

ACKNOWLEDGEMENTS

The authors would like to thank Michael Worley from the Department of Scientific Publications for carefully reviewing this manuscript. We would like to thank Dr. Juri Gelovani for allowing us to use the Xenogen IVIS facility. Also, would like to thank Prof. Yeup Yoon from Mogam Biotechnology Research Institute, Yongin-city, Republic of Korea for providing various NGAL constructs.

Grant support: This work was supported in part by AGA Mentors Research Scholar Award (to SG), UTMDACC Physician Scientist Program Award (to SG), NIH 2P30DK56338 (PFS to SG), and NIH 5P30CA16672 (CCSG to UTMDACC).

REFERENCES

1. Flower DR. The lipocalin protein family: structure and function. Biochem J 1996;318(Pt 1):1–14. [PubMed: 8761444]
2. Kjeldsen L, Bainton DF, Sengelov H, Borregaard N. Identification of neutrophil gelatinase-associated lipocalin as a novel matrix protein of specific granules in human neutrophils. Blood 1994;83:799–807. [PubMed: 8298140]
3. Nielsen BS, Borregaard N, Bundgaard JR, Timshel S, Sehested M, Kjeldsen L. Induction of NGAL synthesis in epithelial cells of human colorectal neoplasia and inflammatory bowel diseases. Gut 1996;38:414–420. [PubMed: 8675096]
4. Borregaard N, Cowland JB. Neutrophil gelatinase-associated lipocalin, a siderophore-binding eukaryotic protein. Biometals 2006;19:211–215. [PubMed: 16718606]
5. Mori K, Lee HT, Rapoport D, et al. Endocytic delivery of lipocalin-siderophoreiron complex rescues the kidney from ischemia-reperfusion injury. J Clin Invest 2005;115:610–621. [PubMed: 15711640]
6. Tong Z, Wu X, Ovcharenko D, Zhu J, Chen CS, Kehrer JP. Neutrophil gelatinase-associated lipocalin as a survival factor. Biochem J 2005;391:441–448. [PubMed: 16060857]
7. Bartsch S, Tschesche H. Cloning and expression of human neutrophil lipocalin cDNA derived from bone marrow and ovarian cancer cells. FEBS Lett 1995;357:255–259. [PubMed: 7835423]
8. Lim R, Ahmed N, Borregaard N, et al. Neutrophil gelatinase-associated lipocalin (NGAL) an early-screening biomarker for ovarian cancer: NGAL is associated with epidermal growth factor-induced epithelio-mesenchymal transition. Int J Cancer 2007;120:2426–2434. [PubMed: 17294443]
9. Stoesz SP, Friedl A, Haag JD, Lindstrom MJ, Clark GM, Gould MN. Heterogeneous expression of the lipocalin NGAL in primary breast cancers. Int J Cancer 1998;79:565–572. [PubMed: 9842963]
10. Hanai J, Mammoto T, Seth P, et al. Lipocalin 2 diminishes invasiveness and metastasis of Ras-transformed cells. J Biol Chem 2005;280:13641–13647. [PubMed: 15691834]
11. Lee HJ, Lee EK, Lee KJ, Hong SW, Yoon Y, Kim JS. Ectopic expression of neutrophil gelatinase-associated lipocalin suppresses the invasion and liver metastasis of colon cancer cells. Int J Cancer 2006;118:2490–2497. [PubMed: 16381001]

12. Playford RJ, Belo A, Poulsom R, et al. Effects of mouse and human lipocalin homologues 24p3/lcn2 and neutrophil gelatinase-associated lipocalin on gastrointestinal mucosal integrity and repair. Gastroenterology 2006;131:809–817. [PubMed: 16952550]
13. Bauer M, Eickhoff JC, Gould MN, Mundhenke C, Maass N, Friedl A. Neutrophil gelatinase-associated lipocalin (NGAL) is a predictor of poor prognosis in human primary breast cancer. Breast Cancer Res Treat 2008;108:389–397. [PubMed: 17554627]
14. Argani P, Rosty C, Reiter RE, et al. Discovery of new markers of cancer through serial analysis of gene expression: prostate stem cell antigen is overexpressed in pancreatic adenocarcinoma. Cancer Res 2001;61:4320–4324. [PubMed: 11389052]
15. Furutani M, Arii S, Mizumoto M, Kato M, Imamura M. Identification of a neutrophil gelatinase-associated lipocalin mRNA in human pancreatic cancers using a modified signal sequence trap method. Cancer Lett 1998;122:209–214. [PubMed: 9464512]
16. Han H, Bearss DJ, Browne LW, Calaluce R, Nagle RB, Von Hoff DD. Identification of differentially expressed genes in pancreatic cancer cells using cDNA microarray. Cancer Res 2002;62:2890–2896. [PubMed: 12019169]
17. Iacobuzio-Donahue CA, Ashfaq R, Maitra A, et al. Highly expressed genes in pancreatic ductal adenocarcinomas: a comprehensive characterization and comparison of the transcription profiles obtained from three major technologies. Cancer Res 2003;63:8614–8622. [PubMed: 14695172]
18. Laurell H, Bouisson M, Berthelemy P, et al. Identification of biomarkers of human pancreatic adenocarcinomas by expression profiling and validation with gene expression analysis in endoscopic ultrasound-guided fine needle aspiration samples. World J Gastroenterol 2006;12:3344–3351. [PubMed: 16733850]
19. Missiaglia E, Blaveri E, Terris B, et al. Analysis of gene expression in cancer cell lines identifies candidate markers for pancreatic tumorigenesis and metastasis. Int J Cancer 2004;112:100–112. [PubMed: 15305381]
20. Gronborg M, Bunkenborg J, Kristiansen TZ, et al. Comprehensive proteomic analysis of human pancreatic juice. J Proteome Res 2004;3:1042–1055. [PubMed: 15473694]
21. Jemal A, Siegel R, Ward E, Murray T, Xu J, Thun MJ. Cancer statistics, 2007. CA Cancer J Clin 2007;57:43–66. [PubMed: 17237035]
22. Furukawa T, Duguid WP, Rosenberg L, Viallet J, Galloway DA, Tsao MS. Long-term culture and immortalization of epithelial cells from normal adult human pancreatic ducts transfected by the E6E7 gene of human papilloma virus 16. Am J Pathol 1996;148:1763–1770. [PubMed: 8669463]
23. Guha S, Eibl G, Kisfalvi K, et al. Broad-spectrum G protein-coupled receptor antagonist, [D-Arg1,D-Trp5,7,9,Leu11]SP: a dual inhibitor of growth and angiogenesis in pancreatic cancer. Cancer Res 2005;65:2738–2745. [PubMed: 15805273]
24. Gray MJ, Van Buren G, Dallas NA, et al. Therapeutic targeting of neuropilin-2 on colorectal carcinoma cells implanted in the murine liver. J Natl Cancer Inst 2008;100:109–120. [PubMed: 18182619]
25. Kunnumakkara AB, Guha S, Krishnan S, Diagaradjane P, Gelovani J, Aggarwal BB. Curcumin potentiates antitumor activity of gemcitabine in an orthotopic model of pancreatic cancer through suppression of proliferation, angiogenesis, and inhibition of nuclear factor-kappaB-regulated gene products. Cancer Res 2007;67:3853–3861. [PubMed: 17440100]
26. Cox BD, Natarajan M, Stettner MR, Gladson CL. New concepts regarding focal adhesion kinase promotion of cell migration and proliferation. J Cell Biochem 2006;99:35–52. [PubMed: 16823799]
27. Venkatesha S, Hanai J, Seth P, Karumanchi SA, Sukhatme VP. Lipocalin 2 antagonizes the proangiogenic action of ras in transformed cells. Mol Cancer Res 2006;4:821–829. [PubMed: 17114340]
28. Mishra J, Mori K, Ma Q, et al. Amelioration of ischemic acute renal injury by neutrophil gelatinase-associated lipocalin. J Am Soc Nephrol 2004;15:3073–3082. [PubMed: 15579510]
29. Fernandez CA, Yan L, Louis G, Yang J, Kutok JL, Moses MA. The matrix metalloproteinase-9/neutrophil gelatinase-associated lipocalin complex plays a role in breast tumor growth and is present in the urine of breast cancer patients. Clin Cancer Res 2005;11:5390–5395. [PubMed: 16061852]
30. Bardeesy N, DePinho RA. Pancreatic cancer biology and genetics. Nat Rev Cancer 2002;2:897–909. [PubMed: 12459728]

31. Gruvberger S, Ringner M, Chen Y, et al. Estrogen receptor status in breast cancer is associated with remarkably distinct gene expression patterns. Cancer Res 2001;61:5979–5984. [PubMed: 11507038]
32. Algul H, Treiber M, Lesina M, Schmid RM. Mechanisms of disease: chronic inflammation and cancer in the pancreas--a potential role for pancreatic stellate cells? Nat Clin Pract Gastroenterol Hepatol 2007;4:454–462. [PubMed: 17667994]
33. Li EM, Xu LY, Cai WJ, Xiong HQ, Shen ZY, Zeng Y. [Functions of neutrophil gelatinase-associated lipocalin in the esophageal carcinoma cell line SHEEC]. Sheng Wu Hua Xue Yu Sheng Wu Wu Li Xue Bao (Shanghai) 2003;35:247–254. [PubMed: 12621549]
34. Duxbury MS, Ito H, Zinner MJ, Ashley SW, Whang EE. Focal adhesion kinase gene silencing promotes anoikis and suppresses metastasis of human pancreatic adenocarcinoma cells. Surgery 2004;135:555–562. [PubMed: 15118593]
35. Baril P, Gangeswaran R, Mahon PC, et al. Periostin promotes invasiveness and resistance of pancreatic cancer cells to hypoxia-induced cell death: role of the beta4 integrin and the PI3k pathway. Oncogene 2007;26:2082–2094. [PubMed: 17043657]
36. Ho QT, Kuo CJ. Vascular endothelial growth factor: biology and therapeutic applications. Int J Biochem Cell Biol 2007;39:1349–1357. [PubMed: 17537667]
37. Korc M. Pathways for aberrant angiogenesis in pancreatic cancer. Mol Cancer 2003;2:8. [PubMed: 12556241]
38. Katz MH, Bouvet M, Takimoto S, Spivack D, Moossa AR, Hoffman RM. Selective antimetastatic activity of cytosine analog CS-682 in a red fluorescent protein orthotopic model of pancreatic cancer. Cancer Res 2003;63:5521–5525. [PubMed: 14500389]
39. Katz MH, Bouvet M, Takimoto S, Spivack D, Moossa AR, Hoffman RM. Survival efficacy of adjuvant cytosine-analogue CS-682 in a fluorescent orthotopic model of human pancreatic cancer. Cancer Res 2004;64:1828–1833. [PubMed: 14996746]
40. Katz MH, Takimoto S, Spivack D, Moossa AR, Hoffman RM, Bouvet M. A novel red fluorescent protein orthotopic pancreatic cancer model for the preclinical evaluation of chemotherapeutics. J Surg Res 2003;113:151–160. [PubMed: 12943825]
41. Caramuta S, De Cecco L, Reid JF, et al. Regulation of lipocalin-2 gene by the cancer chemopreventive retinoid 4-HPR. Int J Cancer 2006;119:1599–1606. [PubMed: 16671099]
42. Berger T, Togawa A, Duncan GS, et al. Lipocalin 2-deficient mice exhibit increased sensitivity to Escherichia coli infection but not to ischemia-reperfusion injury. Proc Natl Acad Sci U S A 2006;103:1834–1839. [PubMed: 16446425]

A.

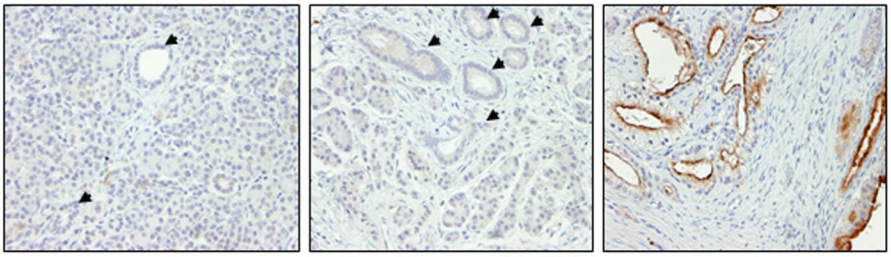

	NGAL		
	Negative (-)	Positive (+)	Total
Normal + CP	57 (74%)	20 (26%)	77
PaCa	40 (54.8%)	33* (45.2%)	73
	* P = 0.0167 (Fisher's test)		

B.

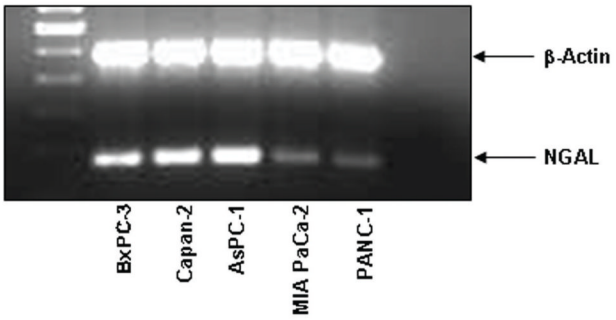

C.

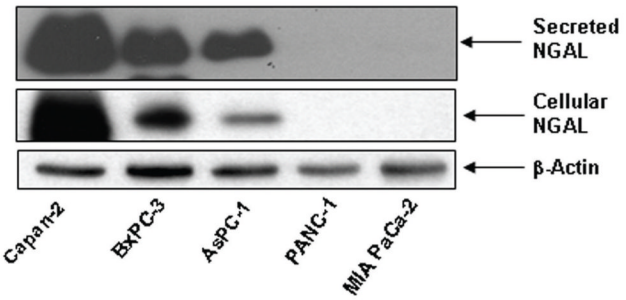

Figure 1. NGAL expression in PaCa tissue and PaCa cells

A. Tissue microarrays from human PaCa (MDACC) were immunohistochemically stained by using a monoclonal NGAL antibody as described in *Materials and Methods.* The table shows a summary of NGAL IHC of the PaCa tissue microarrays. **B**. RT-PCR for NGAL expression by using NGAL-specific primers after total RNA extraction from PaCa cells as described in *Materials and Methods*. C. NGAL expression were determined by western blots of protein lysates or culture media from PaCa cells as described in *Materials and Methods*.

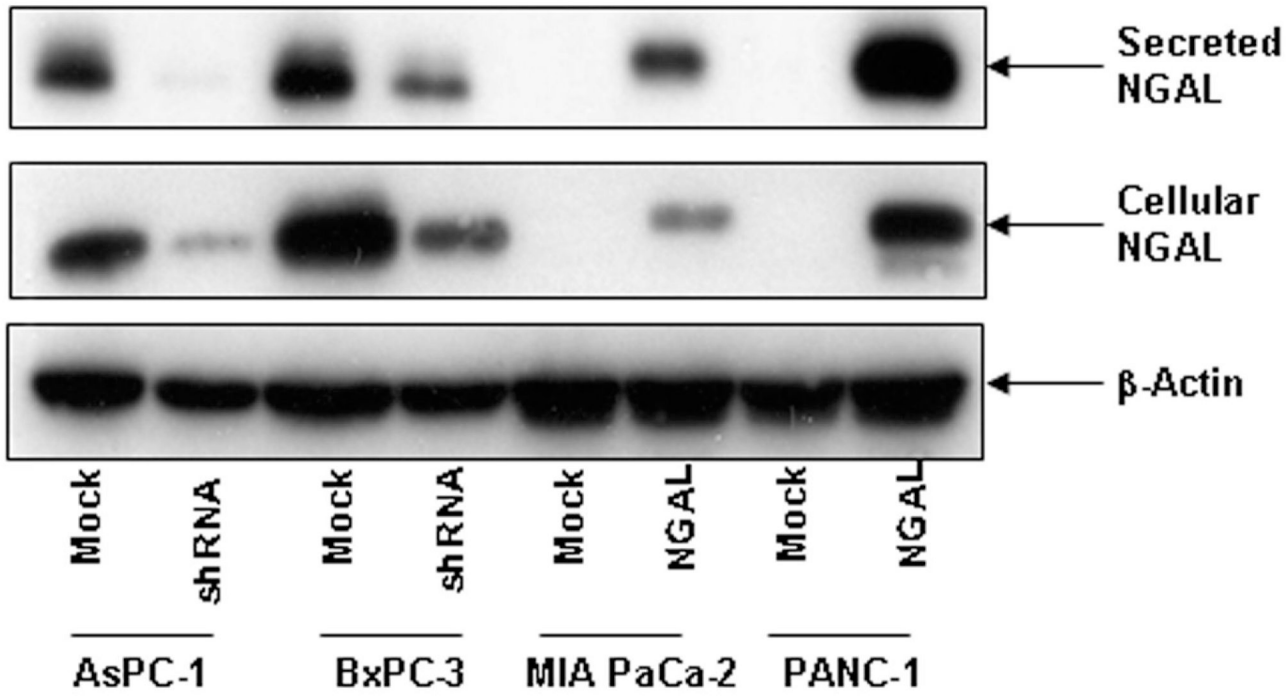

Figure 2. Validation of NGAL expression in stably transformed PaCa cells

Western blots show the expression and secretion of NGAL in stable PaCa cells either overexpressing NGAL or NGAL-shRNA as described in *Materials and Methods*.

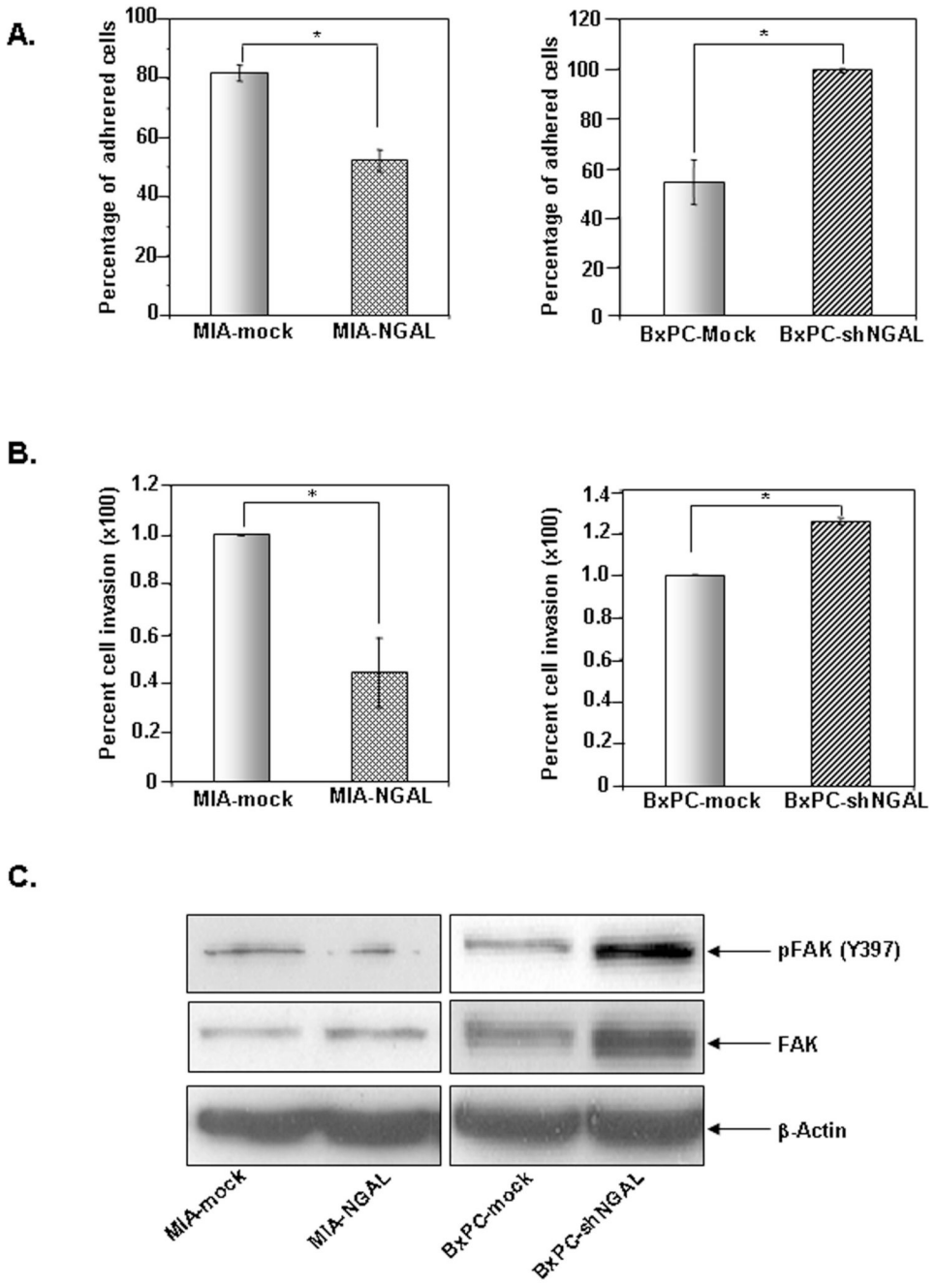

Figure 3. Effects of NGAL on PaCa cell adhesion and invasion

A. Cell suspension (1×10^5/ml) in culture medium either overexpressing NGAL *(left panel)* or NGAL-shRNA *(right panel)* was injected into an adhesion chamber coated with fibronectin. After 10 minutes, adhered cells were counted under a microscope, and the adhesion rate (percentage of adhered cells) was determined as described in *Materials and Methods*. **B**. Cells (1×10^5) overexpressing NGAL *(left panel)* or NGAL-shRNA *(right panel)* were seeded onto a Matrigel™-coated invasion chamber; 16 h later, invaded cells that adhered on the lower surface of the membrane were fixed, stained with Diff Quick set, and counted under a microscope as described in *Materials and Methods*. Representative fields are shown in Suppl. Fig. 1A. Values shown are means ± SE of 3 independent experiments performed in triplicate.

* $P < 0.05$. **C**. Western blots showing phospho-FAK levels in the PaCa cells stably expressing either NGAL or NGAL-shRNA as described in *Materials and Methods*.

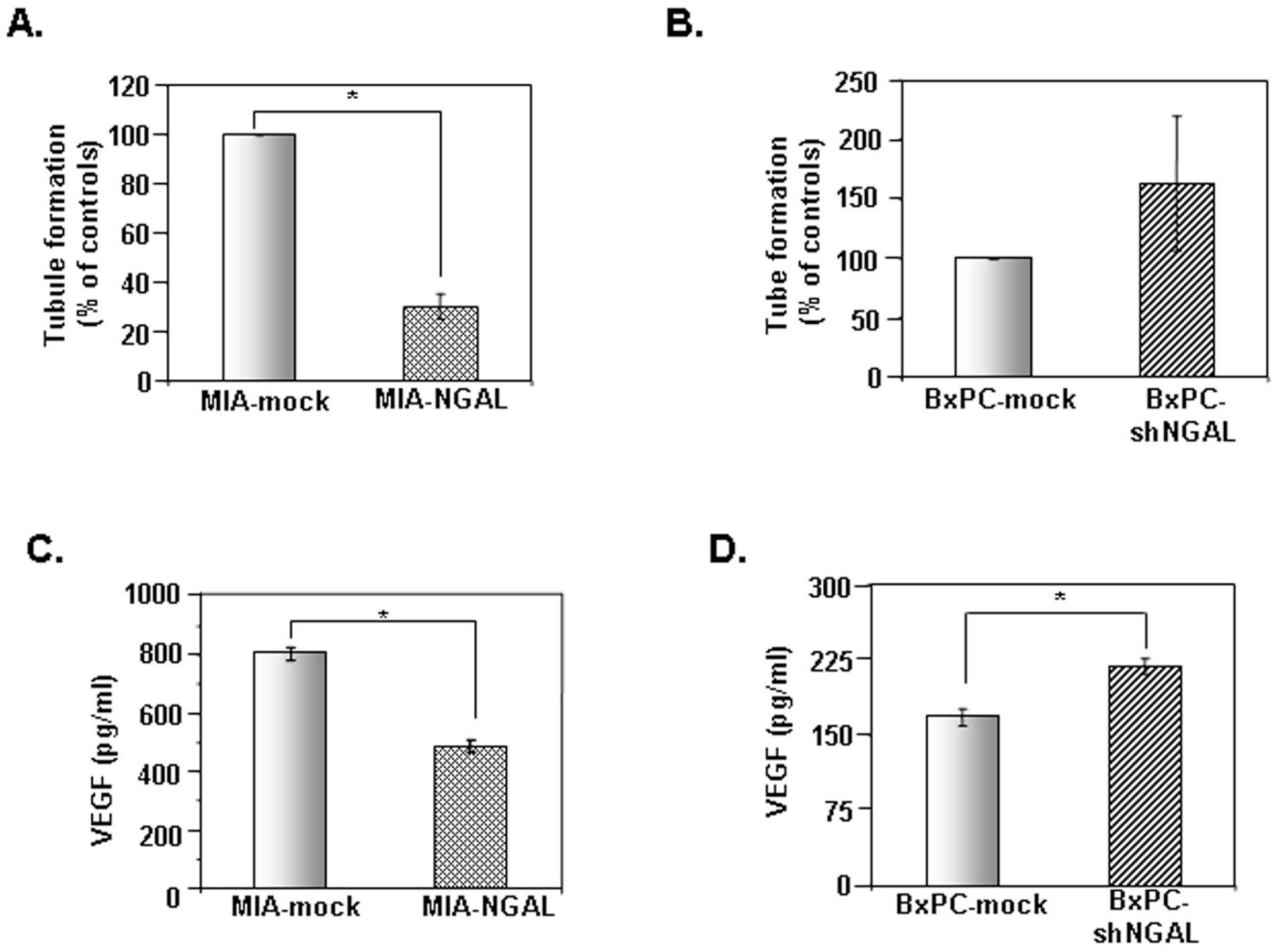

Figure 4. Effects of NGAL on PaCa angiogenesis and VEGF secretion

A and B. HUVEC cells in a conditioned medium from PaCa cells overexpressing NGAL (**A**) or NGAL-shRNA (**B**) and their controls were seeded onto the Matrigel™-coated plate and incubated for 16 h. The tube formation was photographed and counted under a microscope as described in *Materials and Methods*. Representative fields are shown in Suppl. Fig. 2A. The results are expressed as the percentage of the control. **C and D**. The levels of VEGF in culture medium from PaCa cells overexpressing NGAL (**C**) or NGALshRNA (**D**) and their controls were detected by ELISA as described in *Materials and Methods*. Values are means ± SE of 3 independent experiments performed in duplicate. **P* < 0.05.

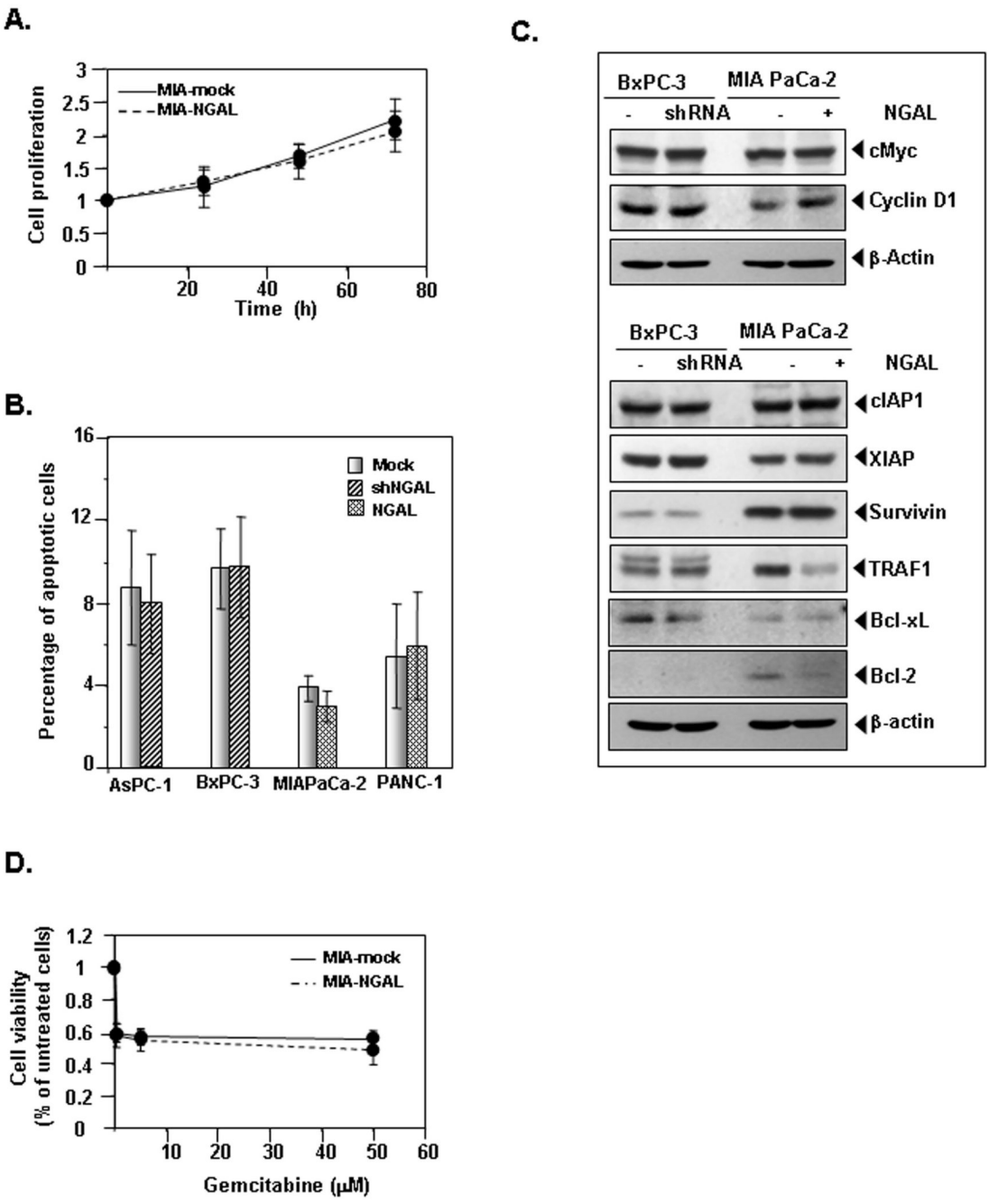

Figure 5. Effects of NGAL on proliferation, apoptosis, and the sensitivity of PaCa cells to chemotherapy

A. PaCa cells proliferation overexpressing NGAL or NGAL-shRNA (Suppl. Fig. 3A) was determined by using the CellTiter Aqueous One Solution Cell Proliferation Assay kit as described in *Materials and Methods*. **B**. PaCa cells apoptosis was determined by flow cytometry with Annexin V-FITC staining as described in *Materials and Methods*. **C**. Western blots show the expression of cell proliferation- and apoptosis-related proteins in stable PaCa cells that overexpress either NGAL or NGALshRNA. **D**. Cells were treated with gemcitabine at indicated doses for 72 h in MIANGAL and control cells or 48 h in BxPC-shNGAL and control cells (Suppl. Fig. 3B). The viability of cells was measured by using the CellTiter

Aqueous One Solution Cell Proliferation Assay kit as described in *Materials and Methods*. Values are means ± SE of 3 independent experiments.

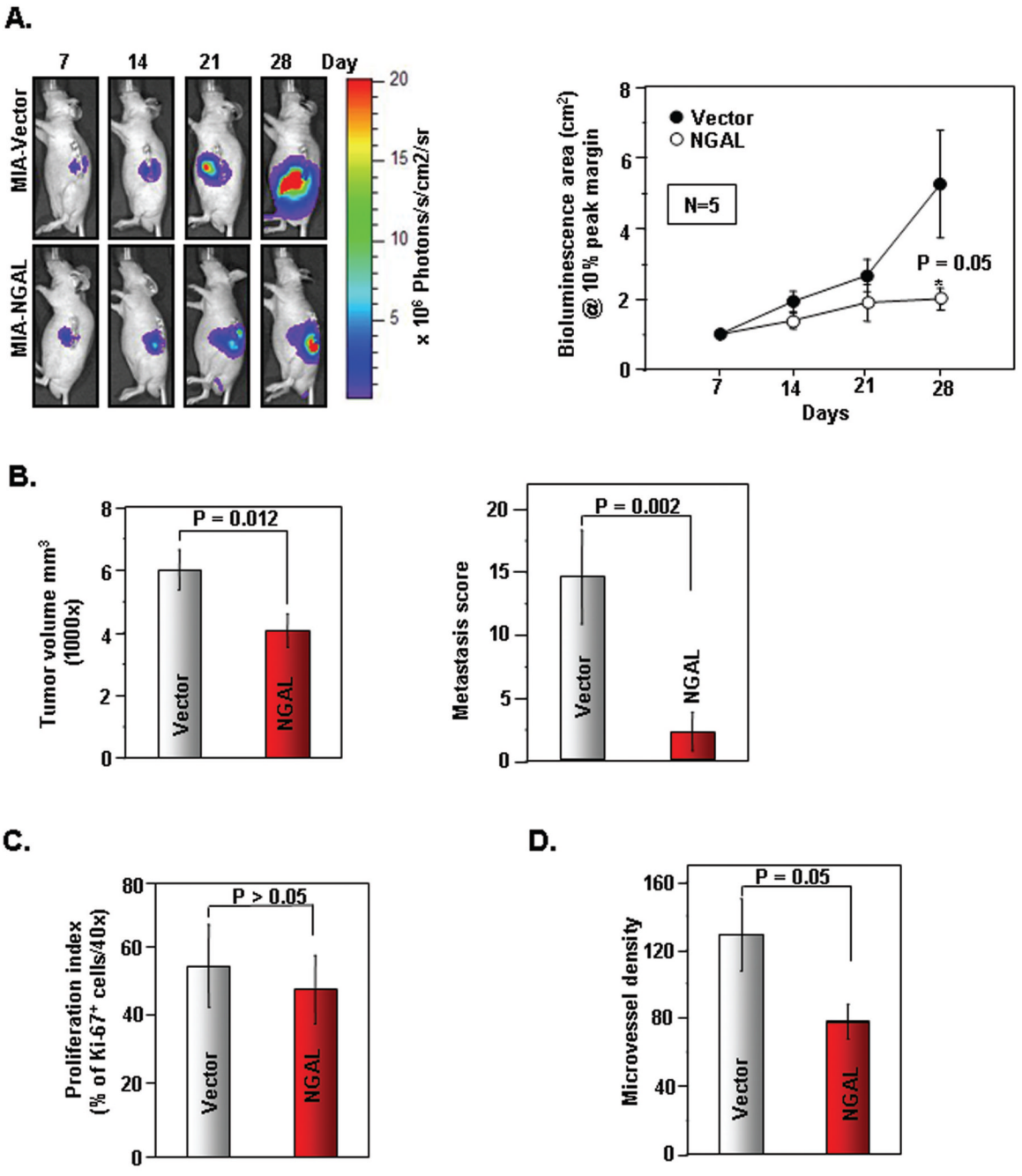

Figure 6. Effects of NGAL on the growth of PaCa tumor and metastases *in vivo*

A. *(Left panel)*, Representative bioluminescence images of orthotopically implanted PaCa in live, anesthetized mice using Xenogen IVIS as described in *Materials and Methods*. *(Right panel)*, Measurements of photons/sec/cm^2/steridian depicting bioluminescence area @10% peak margin (mean ± SE) at indicated time points using Xenogen IVIS as described in *Materials and Methods (n=5)*. *$P < 0.05$. **B**. *(Left panel)*, Final tumor volumes (mean ± SE) measured on 35th day after orthotopic implantation of PaCa cells at autopsy using Vernier calipers and calculated using the formula $V = 2/3\ \pi r^3$ *(n=5)*. *$P < 0.05$. *(Right panel)*, The metastasis score was calculated during autopsy and the composite score was shown in the figure (mean ± SE) as described in *Materials and Methods (n=5)*. *$P < 0.05$. **C**. Quantification of Ki-67$^+$ cells as

described in *Materials and Methods (n=5)*. Values are means ± SE. *$P < 0.05$. Representative Ki-67^+ IHC is shown in Suppl. Fig. 4C. **D**. Quantification of $CD31^+$ microvessel density as described in *Materials and Methods (n=5)*. Values are means ± SE of 3 independent experiments. *$P < 0.05$. Representative $CD31^+$ IHC is shown in Suppl. Fig. 4C.